Article

Effect of Oxygen Nonstoichiometry on the Electrical Conductivity and Thermopower of the $Gd_{0.2}Sr_{0.8}FeO_{3-\delta}$ Ferrite Samples

Vyacheslav Dudnikov[1], Yury Orlov[1], Aleksandr Fedorov[1,2,*], Leonid Solov'yov[3], Sergey Vereshchagin[3], Alexander Burkov[4], Sergey Novikov[3] and Sergey Ovchinnikov[1,2];

[1]Kirensky Institute of Physics, Federal Research Center "Krasnoyarsk Scientific Center, Russian Academy of Sciences, Siberian Branch", Krasnoyarsk, 660036 Russia

[2]Siberian Federal University, Institute of Engineering Physics and Radio Electronics, Krasnoyarsk, 660041 Russia

[3]Institute of Chemistry and Chemical Technology, Federal Research Center "Krasnoyarsk Scientific Center, Russian Academy of Sciences, Siberian Branch", Krasnoyarsk, 660036 Russia

[4]Ioffe Physicotechnical Institute, Russian Academy of Sciences, St. Petersburg, 194021 Russia

* Correspondence: alex99@iph.krasn.ru; Tel.: +7904-898-5175

Received: date; Accepted: date; Published: date

Abstract—The behavior of electrical resistance and thermopower of the $Gd_{0.2}Sr_{0.8}FeO_{3-\delta}$ ferrite samples with the perovskite structure and their stability in the inert gas atmosphere in the temperature range of 300–800 K have been investigated. It has been established that, in the temperature range of interest, the thermoelectric properties in the heating–cooling mode stabilize at $\delta \geq 0.21$. Temperature dependences of the electrical resistance obtained at different δ values have been shown to obey the activation law up to the temperatures of active removal of oxygen from the sample. As the temperature increases, the semiconductor–semiconductor electronic transitions with the activation energy lowering have been observed. The maximum thermoelectric power factor of 0.1 $\mu W/(cm \cdot K^2)$ has been obtained at T = 800 K.

Keywords: substituted rare earth cobalt oxides; stability, thermoelectric properties.

1. Introduction

The main quantities that characterize the properties, quality, and application efficiency of a thermoelectric material are the thermoelectric efficiency $Z = S^2\sigma/\varkappa$ (S is the Seebeck coefficient also known as thermopower, σ is the electrical conductivity, and $\varkappa$ is the thermal conductivity) [1], dimensionless thermoelectric quality factor ZT (T is the absolute temperature), and power factor $P = S^2\sigma = S^2/\rho$ (ρ is the electrical resistivity).

Recently, close attention of researchers has been paid to oxide materials [2], which are stable against high temperatures, nontoxic, and, as a rule, do not contain rare elements. A group of complex oxides of the rare-earth transition metals $Ln_{1-x}A_xMO_{3-\delta}$ (Ln is lanthanoid, A is alkali or alkali-earth metal, and M is transition metal (Co, Fe, or Mn) with the perovskite structure holds a special place [3,4] [5] among the oxides promising for application. The diversity of physicochemical properties of these compounds belonging to the systems with the strong electron correlations are interesting not only for application [6], but also for fundamental research. Along with the thermoelectric characteristics, of great importance is the stability of these materials under different environmental conditions, including the atmospheric composition and temperature. Taking into account the significant differences in the low-temperature

properties of the $Gd_{1-x}Sr_xFeO_{3-\delta}$ compounds with different oxygen nonstoichiometry indices δ [7] and high mobility of oxygen established in the $Gd_{1-x}Sr_xCoO_{3-\delta}$ compounds [8], here we examine the effect of oxygen nonstoichiometry on the thermoelectric properties of the $Gd_{0.2}Sr_{0.8}FeO_{3-\delta}$ compound and its stability in the temperature range of 300–800 K.

2. Experimental

Sample synthesis. The $Gd_{0.2}Sr_{0.8}FeO_{3-\delta}$ samples were obtained by the glycine–nitrate-based solution-combustion synthesis [9]. The initial components of the perovskite oxide were cations of nitrates of each metal component. The initial gel was prepared by evaporation of a glycine–nitrate-based solution at 363 K with subsequent slow heating until combustion. The prepared powder was calcinated in air at 723 K for 5 h, thoroughly grinded in аᴛ agate mortar, and sintered in air at 1523 K for 5 h with subsequent slow cooling to room temperature at a rate of 2 deg/min. Tablets were synthesized at T_c = 1473 K for 24 h and cooled in the same regime.

Oxygen nonstoichiometry of the samples was determined on a NETZSCHSTA449C analyzer equipped with an Aëolos QMS 403C mass spectrometer. The measurements were performed in the 5-% H_2-Ar mixture flow in a corundum crucible with a perforated cover; the sample mass was 30 mg. The oxygen content in the $Gd_{0.2}Sr_{0.8}FeO_{3-\delta}$ samples was determined from the mass decrement Δ*m* using the equation $\delta(T) = \delta_0 + M\Delta m(T)/1600$, where $\delta(T)$ is the δ value at temperature *T*, $\Delta m(T)$ (%) is the mass decrement at this temperature, and *M* is the molecular mass of $Gd_{0.2}Sr_{0.8}FeO_{2.87}$. The measurement error was δ = ±0.01. The oxygen nonstoichiometry index of the initial $Sr_{0.8}Gd_{0.2}FeO_{3-\delta}$ material was taken to be δ_0 = 0.13 in accordance with the data on the Gd-Sr-Fe perovskite synthesized by the same technique in [10].

X-ray diffraction measurements were performed on a PANalytical X'Pert PRO powder diffractometer (Netherlands) in Co*K*α radiation in the 2θ angle range of 10–90°. The crystal lattice and structure were refined by the full profile analysis of X-ray diffraction patterns using the derivative difference minimization (DDM) method [11]. Temperature dependences of the thermopower and electrical resistance were obtained on an experimental setup developed at the Ioffe Institute, St. Petersburg [12,13].

3. Results and discussion

In contrast to the complex cobalt oxides $Re_{1-x}Sr_xCoO_{3-\delta}$ (Re is the rare-earth ion), which, depending on the cooling rate and synthesis temperature, can form compounds ordered or disordered over the perovskite structure A sites [14] [15] [16] [17][S18] [19], the $Gd_{0.2}Sr_{0.8}FeO_{3-\delta}$ compound synthesized by us is disordered and characterized by the random distribution of oxygen vacancies and cations over the A sites. The X-ray diffraction study revealed no foreign phases. According to the X-ray powder diffraction data (Fig. 1), the synthesized $Gd_{0.2}Sr_{0.8}FeO_{3-\delta}$ samples, similar to the heavily-doped $La_{1-x}Sr_xFeO_{3-\delta}$ (0.8 ≤ x ≤ 1.0) compounds [20], have a form of a disordered perovskite with the cubic symmetry (sp. gr. *Pm*3*m* (*a* = 3.8856(2) Å), in which all the iron sites are identical, as in the mixed-valence iron compounds $Sr_2LaFe_3O_{8.94}$ [21].

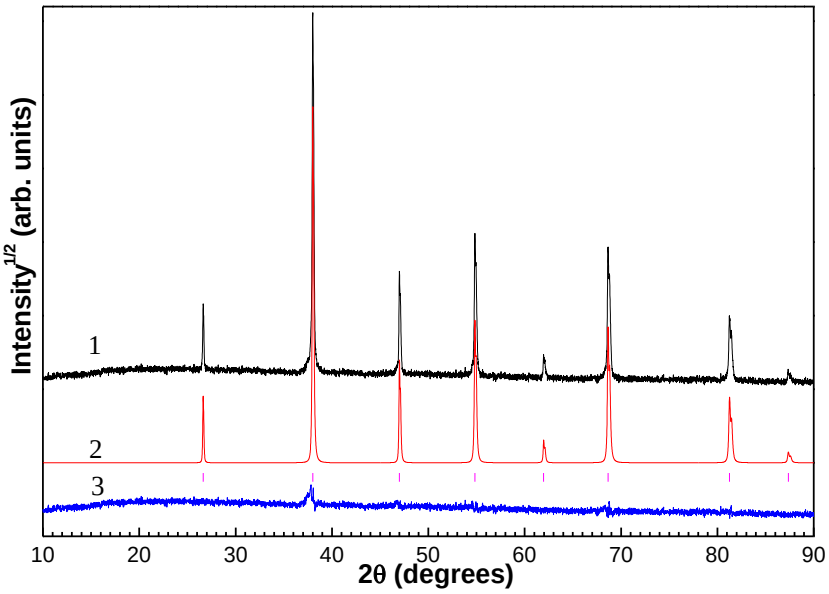

Fig. 1. (1) Experimental, (2) calculated, (3) and difference X-ray diffraction patterns of the Gd $_{0.2}Sr_{0.8}FeO_{3-\delta}$ compound after the DDM refinement.

Figure 2 shows the temperature-programmed reduction data. The change in the mass caused by removal of oxygen from the sample upon heating in the 5%H_2-Ar reducing atmosphere starts at ~500 K and depends on the heating rate, which is related to the solid-state reduction kinetics. As the heating rate increases, the thermogravimetric (TG) and derivative thermogravimetric (DTG) curves shift to the high-temperature region and the maximum reduction rate is observed at 640 and 725 K at heating rates of 2 and 20 K/min, respectively.

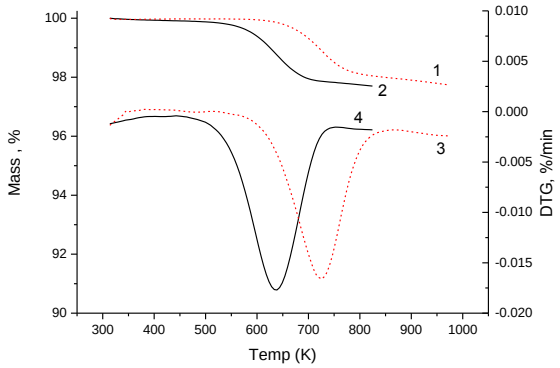

Fig. 2. (1, 2) TG and (3, 4) DTG curves of temperature-programmed reduction of the Gd $_{0.2}Sr_{0.8}FeO_{2.87}$ compound in the 5-% H_2-Ar mixture flow at heating rates of 2 (black solid curve) and 20 K/min (red dotted curve).

The electrical resistivity and thermopower were measured on the rectangular bar samples 0.9 × 4.5 × 9 mm in size at temperatures from 300 to 800 K in the inert He (99.999%) atmosphere. To examine the changes in the temperature dependences of the resistivity and thermopower, the measurements were performed during the heating–cooling cycles and the courses of the obtained temperature curves were compared. Three thermal cycles were performed. The heating and cooling rates were 5 deg/min. The results obtained are shown in Fig. 3. It can be seen that the temperature dependences of the electrical resistivity and thermopower of the investigated samples in the heating–cooling cycles are essentially different, which is indicative of the strong effect of oxygen on the physical properties of the Gd $_{0.2}Sr_{0.8}FeO_{3-\delta}$ compound. In the first thermocycle, when oxygen is actively removed from the sample, the behavior of the thermoelectric parameters of the compound is especially anomalous (Fig. 4a). For clarity, the electrical resistivity and Seebeck coefficient measured during the first heating with the active oxygen removal (Fig. 4a) and the last cooling (Fig. 4b), when the sample is almost stable, are plotted.

а) б)

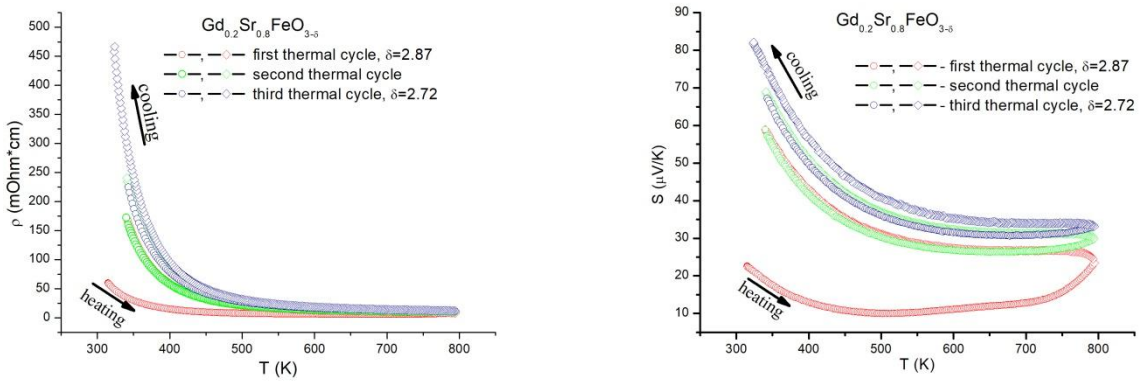

Fig. 3. Temperature dependences of (a) the resistivity and (b) thermopower for three continuous heating–cooling cycles.

а) б)

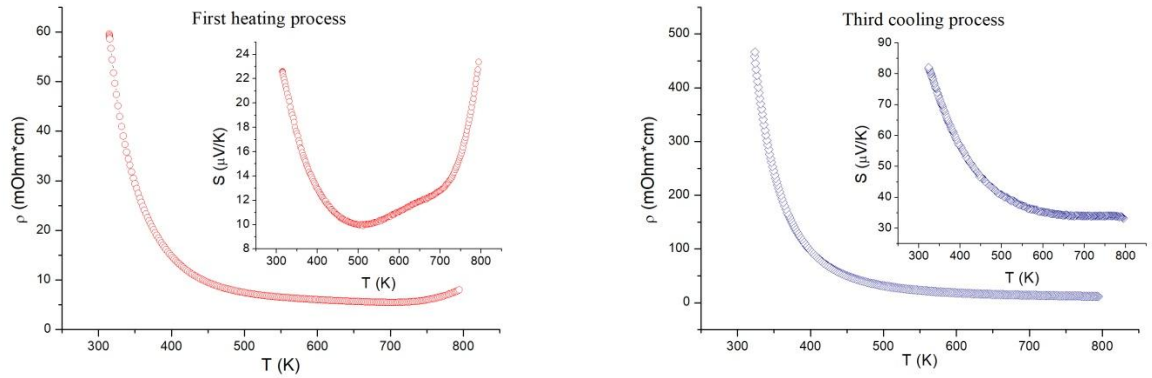

Fig. 4. Temperature dependences of the resistivity and thermopower (insets) during (a) the first heating and (b) the third cooling.

The anomalies in the behavior of the Seebeck coefficient correlate with the data of thermogravimetric analysis at the sample mass loss caused by the removal of oxygen and are observed at much lower temperatures than in the behavior of the resistivity (Fig. 4a).

The oxygen nonstoichiometry index δ increases from one heating–cooling cycle to another and the deviation from the semiconductor-type conductivity shifts toward higher temperatures. At δ = 0.21, the temperature dependence of the resistivity is qualitatively consistent with the semiconductor-type conductivity $d\rho/dT < 0$ over the entire temperature range of interest (Fig. 4b). The conductivity in the regions corresponding to the semiconductor type obeys the thermal activation law $\rho(T) = \rho_0 \cdot \exp(E_a/k_B T)$, where ρ_0 is the coefficient weakly dependent on temperature, $E_a$is the activation energy, and k_B is the Boltzmann constant. The dependences of the logarithmic resistivity of the sample on the reciprocal temperature in the corresponding temperature ranges for several heating and cooling processes are presented in Fig. 5. For all the thermal cycles, the ln(ρ)(1/T) curves contain two portions that are described well by the thermal activation law with different activation energies E_a. At each

specific δ value, the activation energy decreases with increasing temperature. At the same time, the activation energy grows with the oxygen nonstoichiometry index. The absolute values of the oxygen nonstoichiometry indices and activation energies for different temperature ranges and electronic transition temperatures determined as the crossing points of the approximation curves are given in Table 1.

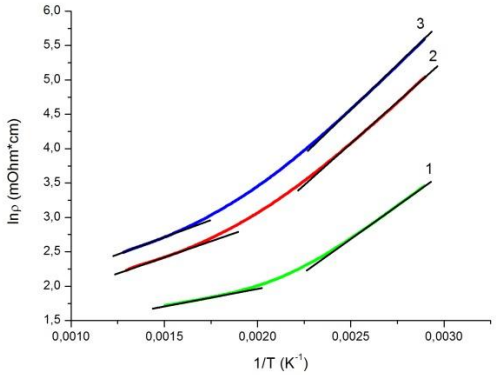

Fig. 5. Reciprocal temperature dependence of the $Gd_{0.2}Sr_{0.8}FeO_{3-\delta}$ logarithmic resistivity. Black straights show the thermal activation law processing. (1) First heating, (2) first cooling, and (3) third cooling.

Figure 6 presents the plots of activation energy E_a in the low-temperature (below the temperature of the electronic transition, $T < T_{p\text{-}p}$) and high-temperature (above the transition temperature, $T > T_{p\text{-}p}$) regions and semiconductor–semiconductor transition temperature $T_{p\text{-}p}$ as functions of the oxygen content in the sample. It can be seen that, in the investigated temperature and δ ranges, all the dependences are linear.

Table 1. Oxygen nonstoichiometry indices, activation energies, and electronic transition temperatures for the $Gd_{0.2}Sr_{0.8}FeO_{3-\delta}$ ferrite sample

	δ	E_a ($T < T_{p\text{-}p}$), eV	$T_{p\text{-}p}$, K	E_a ($T > T_{p\text{-}p}$), eV
1st heating	0.13±0.01	0.16±0.01	461±1	0.04±0.01
1st cooling	0.19±0.01	0.20±0.01	495±1	0.07±0.01
2nd cooling	0.20±0.01	0.21±0.01	502±1	0.08±0.01
3rd cooling	0.21±0.01	0.22±0.01	507±1	0.09±0.01

The E_a value in the low-temperature range is several times higher than in the high-temperature range; the difference slightly decreases with increasing δ. The electrical conductivity of the materials under study is implemented by impurity carriers induced by different-valence Gd+3/Sr+2 cation substitutions and holes related to oxygen vacancies. At high temperatures, we observe the properties of an almost degenerate semiconductor, while at low temperatures, the activation energy increases. The temperature $T_{p\text{-}p}$ of the asymptotic change weakly depends on the vacancy concentration. The fact that the activation energy depends on the vacancy concentration can evidence for the shift of the impurity level from the allowed state band extremum. It is worth noting that the concentration dependences of the activation energies (straights 1 and 2 in Fig. 6) are almost parallel.

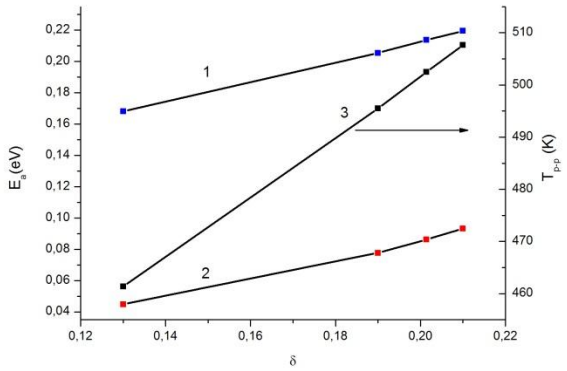

Fig. 6. Dependences of the activation energy E_a (1 is the temperature region below the electronic transition and 2 is the high-temperature region) and (3) semiconductor–semiconductor transition temperature $T_{p\text{-}p}$ on the oxygen nonstoichiometry index.

Figure 7 shows temperature dependences of the power factor P for the first and last temperature cycles. It can be seen that, as the temperature increases, the power factor of the samples grows, yet not attains its maximum, in the investigated temperature range. In the sample stability region, the increase is monotonic, without jumps, and almost linear for the sample with δ = 0.21. At a temperature of T = 500 K, the power factor of the sample with δ = 0.21 exceeds almost fourfold the power factor of the samples with δ = 0.13 (0.052 μW/(K^{2}cm) and 0.013 μW/(K^{2}cm) and the maximum P value obtained at T = 800 K is 0.1 μW/(K^{2}cm).

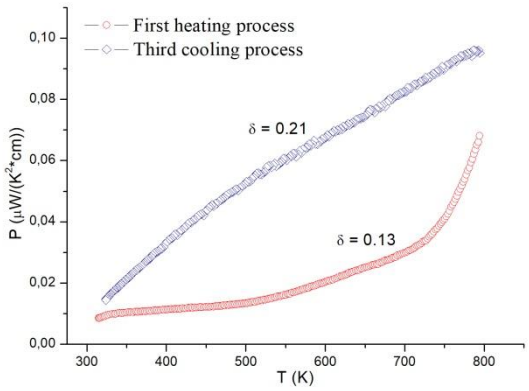

Fig. 7. Temperature dependences of the power factor P for the samples with different oxygen contents.

4. Conclusions

The behavior of electrical resistivity and thermopower of the disordered $Gd_{0.2}Sr_{0.8}FeO_{3-\delta}$ perovskite in the temperature range of 300–800 K and its stability in the helium atmosphere were investigated. It was established that the stability of thermoelectric parameters strongly depends on the oxygen content in a sample and is obtained at temperatures from 300 to 800 K at an oxygen nonstoichiometry index of δ ≥ 0.21.

In the sample stability region, the temperature dependences of electrical resistivity for all δ values contain portions that are described well by the thermal activation law; as the temperature increases, spread semiconductor–semiconductor transitions are observed, which are accompanied by a decrease in the activation energy. The latter grows with decreasing oxygen content in a sample. In this case, the temperature of electronic transition depends linearly on the oxygen nonstoichiometry. The activation energies in the low- and high-temperature regions depend similarly on the δ value.

The increase in the δ value leads to the significant enhancement of the power factor P. In particular, at a temperature of T = 500 K, the power factor of the sample with δ = 0.21 is almost fourfold higher than the power factor of the samples with δ = 0.13 (0.052 μW/(K^{2}cm) and 0.013 μW/(K^{2}cm). In the sample with δ = 0.21, the power factor increases with temperature almost linearly and attains its maximum

value of 0.1 μW/(cm·K^2) at T = 800 K. Thus, varying the oxygen content in a sample, one can control the temperature ranges of stability and power factor of the complex transition metal oxides.

Acknowledgments

This study was supported by the Russian Science Foundation, project no. 16-13-00060.

References

[1] Ioffe A. F., Semiconductor Thermoelements, and Thermoelectric Cooling; London:Infosearch, 1957; Rowe D.M., CRC Handbookof Thermoelectrics; CRC Press, 1995.

[2] Shiand X., Chenand L., Uher C., Recent advances in high-performance bulk thermoelectric materials. International Materials Reviews, 2016, v. 61, 379-415.

[3] Terasaki, Sasago Y., Uchinokura K., Large thermoelectric power in NaCo2O4 single crystals, Phys Rev B: Condens Matter, 1997, 56 , R12685(R), DOI: https://doi.org/10.1103/PhysRevB.56.R12685.

[4] Weidenkaff A., Aguirre M.H., Bocher L., Trottmann M., Tomes P., Robert R., Development of Perovskite-type Cobaltates and Manganates for Thermoelectric Oxide Modules, Journal of the Korean Ceramic Society, 2010, Vol. 47, No. 1, pp. 47-53,. DOI:10.4191/KCERS.2010.47.1.047.

[5] Harizanova S.G., Zhecheva E.N., Valchev V.D., Khristova M.G., Stoyanova R.K., Improving the thermoelectric efficiency of Co based ceramicsm, Materials Today: Proceedings, 2015, 2, 4256 – 4261, doi: 10.1016/j.matpr.2015.09.011.

[6] Zlati´c V., Boyd G. R., Freericks J. K., Phys. Rev. B, 2014, **89**, 155101; Haverkort M.W., Hu Z., Cezar J.C., Burnus T., Hartmann H., Reuther M., Zobel C., Lorenz T., Tanaka A., Brookes N.B., Hsieh H.H., Lin H. J., Chen C.T., Tjeng L.H., Phys. Rev. Lett. , 2006, **97**, 176405.

[7] Blasco J., Stankiewicz J., García J., Phase segregation in the $Gd_{1-x}Sr_xFeO_{3-\delta}$ series, Journal of Solid State Chemistry , 2006, 179, 898‑908, doi:10.1016/j.jssc.2005.12.023.

[8] Vereshchagin S.N., Dudnikov V.A., Solovyov L.A., Study of Mobile Oxygen in Ordered/Disordered Nonstoichiometric Sr-Gd-Cobaltate by Simultaneous Thermal Analysis, Journal of Siberian Federal University. Chemistry, 2017, 3, 10, 346-357, DOI: 10.17516/1998-2836-0031.

[9] Chick L.A., Pederson L.R., Maupin G.D., Bates J.L., Thomas L.E., Экхархос G.J., Матер. Lett., 1990, 10, 6.

[10] Blasco J., Stankiewicz J., Garcıa J., Phase segregation in the $Gd_{1-x}Sr_xFeO_{3-\delta}$ series, Journal of Solid State Chemistry, 2006, 179 , 898–908; doi:10.1016/j.jssc.2005.12.023.

[11] Solovyov L. A., Full-Profile Refinement by Derivative Difference Minimization, J. Appl. Crystallogr., 2004, 37, 743–749

[12] BurkovA.T. et al., Meas. Sci. Technol., 2001, **12,** 264–272.

[13] Burkov A.T., Fedotov A.I., Kasyanov A.A., Panteleev R.I., Nakama T., Methods and technique of thermopower and electricalconductivity measurements of thermoelectric materials at high temperatures, Scientific and Technical Journal of Information Technologies, Mechanics and Optics, 2015, vol.15, no. 2, pp. 173–195; doi:10.17586/2226-1494-2015-15-2-173-195.

[14] James M., Tedesco T., Cassidy D.J. and R.L. Withers, Materials Research Bulletin, 2005, 40, 990.

[15] James M., Morales L. and K.Wallwork, Physica B ,2006, 199, 385-386.

[16] Vereshchagin S.N., Dudnikov V.A., Shishkina N.N., Solovyov L.A., Phase transformation behavior of $Sr_{0.8}Gd_{0.2}CoO_{3-\delta}$ perovskite in the vicinity of order-disorder transition, Thermochimica Acta, 2017, 655, pp 34–41, https://doi.org/10.1016/j.tca.2017.06.003.

[17] Vereshchagin S.N., Solovyov L.A., Rabchevskii E.V., Dudnikov V.A., Ovchinnikov S.G., Anshits A. G., Methane oxidation over A-site ordered and disordered $Sr_{0.8}Gd_{0.2}CoO_{3-d}$ perovskites, Chem. Commun., 2014. V.50 , P. 6112 – 6115.

[18] . Yoshida, Kobayashi W., Nakano T., Terasaki I., Matsubayashi K., Uwatoko Y., Grigoraviciute I., Karppinen M., Yamauchi H., Chemical and physical pressure effects on the magnetic and transport properties of the A-site ordered perovskite $Sr_3YCo_4O_{10.5}$, Journal of the Physical Society of Japan, 2009, V 78, 094711, DOI: 10.1143/JPSJ.78.094711.

[19] Fukushima S., Sato T., Akahoshi D., Kuwahara H., Comparative study of ordered and disordered $Y_{1-x}Sr_xCoO_{3-\delta}$, J. Appl. Phys., 2008, V 103, 07F705, DOI: 10.1063/1.2830615.

[20] Dann S.E., Currie D.B., Weller M.T., Thomas M.F., Al-Rawwas A.D., The Effect of Oxygen Stoichiometry on Phase Relations and Structure in the System $La_{1-x}Sr_xFeO_{3-\delta}$ (0 <= x <= 1, 0 <= δ <= 0.5), 1994, J Solid State Chem., 1994, V 109, 134 -144. DOI: 10.1006/jssc.1994.1083.

[21] Battle P.D., Gibb T.C., Lightfoot P., The structural consequences of charge disproportionation in mixed-valence iron oxides. The crystal structure of $Sr_2LaFe_3O_{8.94}$ at room temperature and 50 K., J Solid State Chem., 1990, V84., P 271-279. doi.org/10.1016/0022-4596(90)90325-R.